Supplementary Materials for

Spinal cord retinoic acid receptor signaling gates mechanical hypersensitivity in neuropathic pain

Bing Cao[1], Gregory Scherrer[2], Lu Chen[1,3,*]

[1] Department of Neurosurgery, Wu Tsai Neuroscience Institute, Stanford University School of

Medicine, Stanford, CA 94305.

[2] Department of Cell Biology and Physiology, UNC Neuroscience Center, Department of

Pharmacology, University of North Carolina at Chapel Hill, Chapel Hill, NC 27599.

[3] Lead contact

*Correspondence: luchen1@stanford.edu

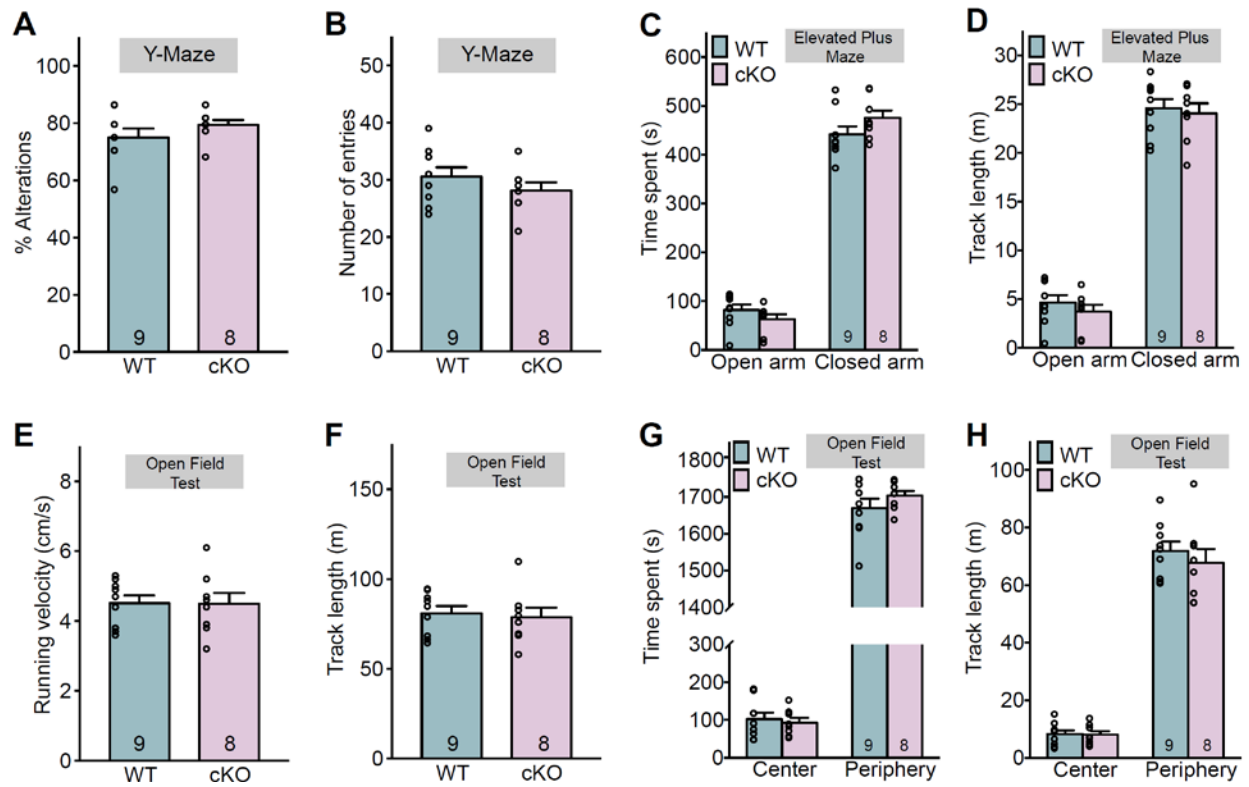**The supplementary materials contain eight supplementary figures**

Figure S1. Behavioral assessment of Y-Maze, elevated plus maze and open field test in wild-type and PV-RARα conditional knock-out mice, related to Figure 1.

(A-B) Quantification of Y-maze test. Percentage of alternations (A) and number of total entries (B) were measured from WT and PV-RARα KO mice.

(C-D) Quantification of Elevated plus maze test. Average time spent (C) and average track length in open or closed arms (D) were measured.

(E-H) Quantification of open field test. Average velocity (E), average track length (F), average time spend (G), and average track length (H) in the center and periphery of the chamber were measured.
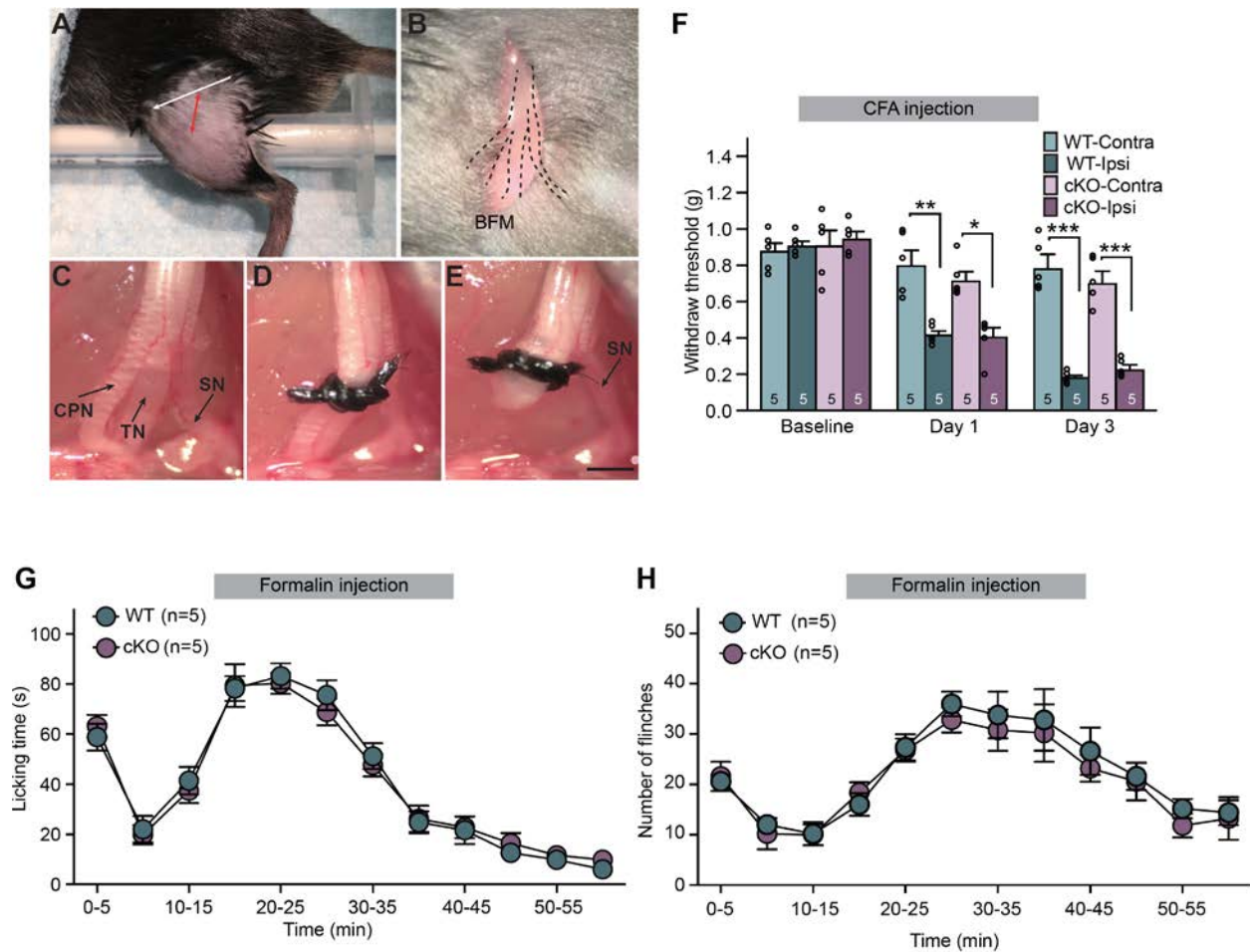
All data represent mean ± SEM.

Figure S2. SNI surgery and assessment of nociceptive behavior through CFA and formalin test in WT and PV-RARα cKO mice, related to Figure 1.

(A-E) SNI surgery. The incision (red line) is made at the middle position of the thigh at a 60° angle from a fictive axe (white line) between trochanter major and iliaca cresta (A). Following the incision along the red line, expose the biceps femoris muscle (BFM) and perform a careful blunt dissection to expose the trifurcation of the sciatic nerve. Dotted lines show the position of the sciatic trifurcation underneath the artery genus descendes and biceps femoris (B). The three bare branches of the sciatic nerve are shown. common peroneal (CPN), tibial (TN) and sural nerves (SN) (C). Ligation of the common peroneal and tibial nerves was performed with a surgical knot (D). The ligated nerves were transected distally for 2 mm section to prevent nerve regeneration. Care was taken to avoid contact with the sural nerve (E). Scale bar: 2mm.

(F) Mechanical allodynia after complete Freund's adjuvant (CFA)-induced inflammation, quantified as withdraw threshold in von Frey test in WT and PV-RARα cKO mice before, 1-day and 3-day after CFA injection. Two-way ANOVA followed by Bonferroni test, day 1: interaction (genotype × CFA), $F_{(1, 16)} = 0.38$, $p = 0.55$; CFA factor, $F_{(1, 16)} = 35.09$, $p < 0.001$; day 3: interaction, $F_{(1, 16)} = 1.32$, $p = 0.27$; CFA factor, $F_{(1, 16)} = 96.84$, $p < 0.001$. Post hoc test, *, $p < 0.05$; **, $p < 0.01$; ***, $p < 0.001$. Data shown as mean ± s.e.m..

(G) Time course of paw licking responses and flinching (H) in WT and PV-RARα cKO mice following injection of 1% formalin (50µl, subcutaneous) under the plantar of left hind paw at T=0. Both WT and cKO mice showed the two characteristic phases of nociceptive behavior: An early phase of high licking/flinch period immediately after formalin injection that lasted approximately 5 min, followed by a lull, and a more prolonged but delayed late phase. Behavioral measurements are binned every 5 minutes (mean ± s.e.m.).
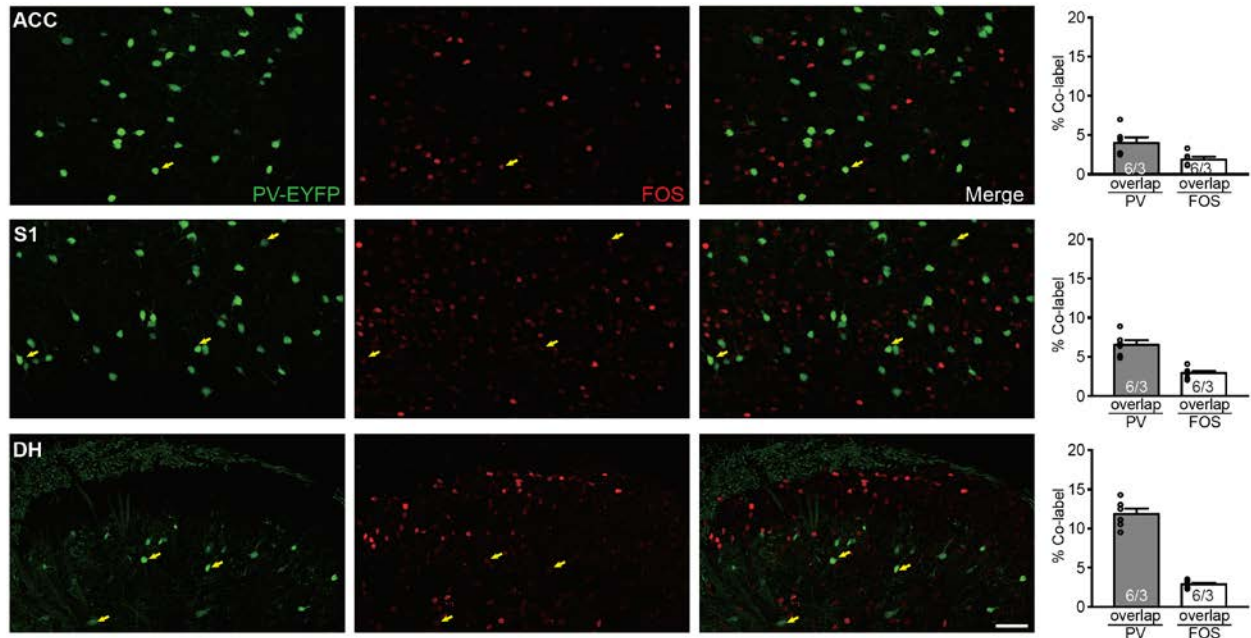
Figure S3. Quantification of FOS-expressing PV+ neurons in cortical regions and spinal cord dorsal horn, related to Figure 2.

Contralateral ACC, S1 and ipsilateral dorsal horn sections were obtained from WT-SNI mice after gentle brush stimulation. Mice also express an EYFP reporter driven by PV-Cre. Percentage of FOS-expressing PV cells and PV+ FOS-expressing cells were quantified for each region (6 sections from 3 mice for each region). Scale bar: 50 μm. All data represent mean ± s.e.m.
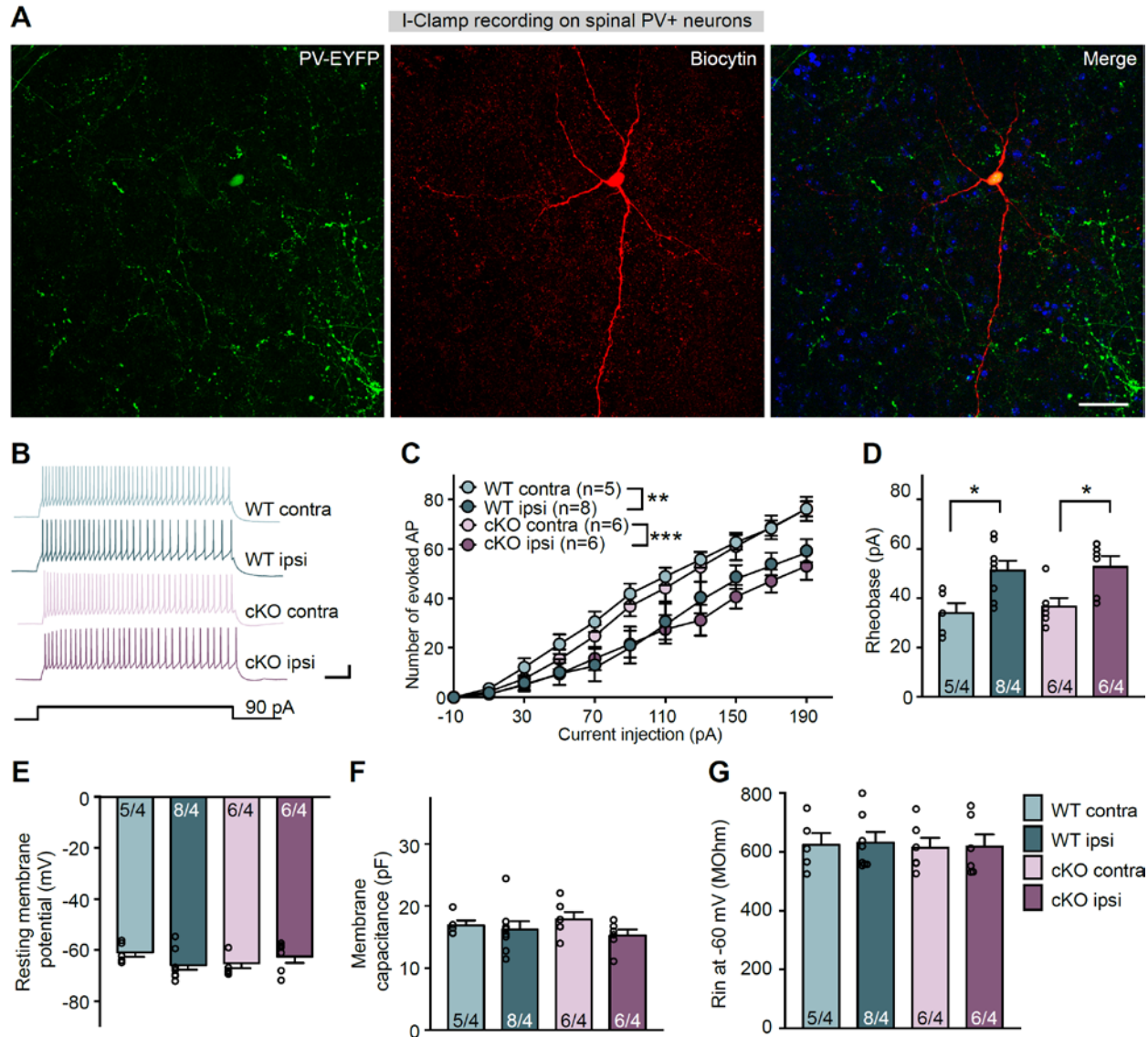
Figure S4. Spared nerve injury affects active membrane properties of PV+ cells in the dorsal horn, related to Figures 4-6.

(A) Representative images of biocytin-labelled (red) PV+ cells, which was identified with Cre-dependent EYFP reporter expression. Scale bar: 50 μm.

(B) Sample traces of current clamp recordings from WT and RARα KO PV+ neurons ipsi- and contralateral to SNI side in response to a step current injection of 90 pA. Scale bars: 100 ms, 10 mV.

(C) Input-output relationships between the total number of APs and the step current injections. Two-way ANOVA followed by Bonferroni test, WT contra vs. ipsi: interaction (intensity × SNI) $F_{(10, 110)} = 2.76$, **, $p < 0.01$; SNI factor, $F_{(1, 11)} = 3.77$, $p = 0.078$; cKO contra vs. ipsi: interaction, $F_{(10, 100)} = 6.34$, ***, $p < 0.01$; SNI factor, $F_{(1, 10)} = 5.73$, $p < 0.05$.

(D) Rheobase of PV+ cells at the ipsilateral and contralateral sides of WT and cKO mice. Two-way ANOVA followed by Tukey test, interaction (genotype × SNI), $F_{(1, 21)} = 0.065$, $p = 0.80$; SNI factor, $F_{(1, 21)} = 18.07$, $p < 0.001$. Post hoc test, *, $p < 0.05$.

(E-G) Quantification of passive membrane properties measured as resting membrane potentials (E), membrane capacitances (F), and input resistances (G) at -60 mV holding potential.
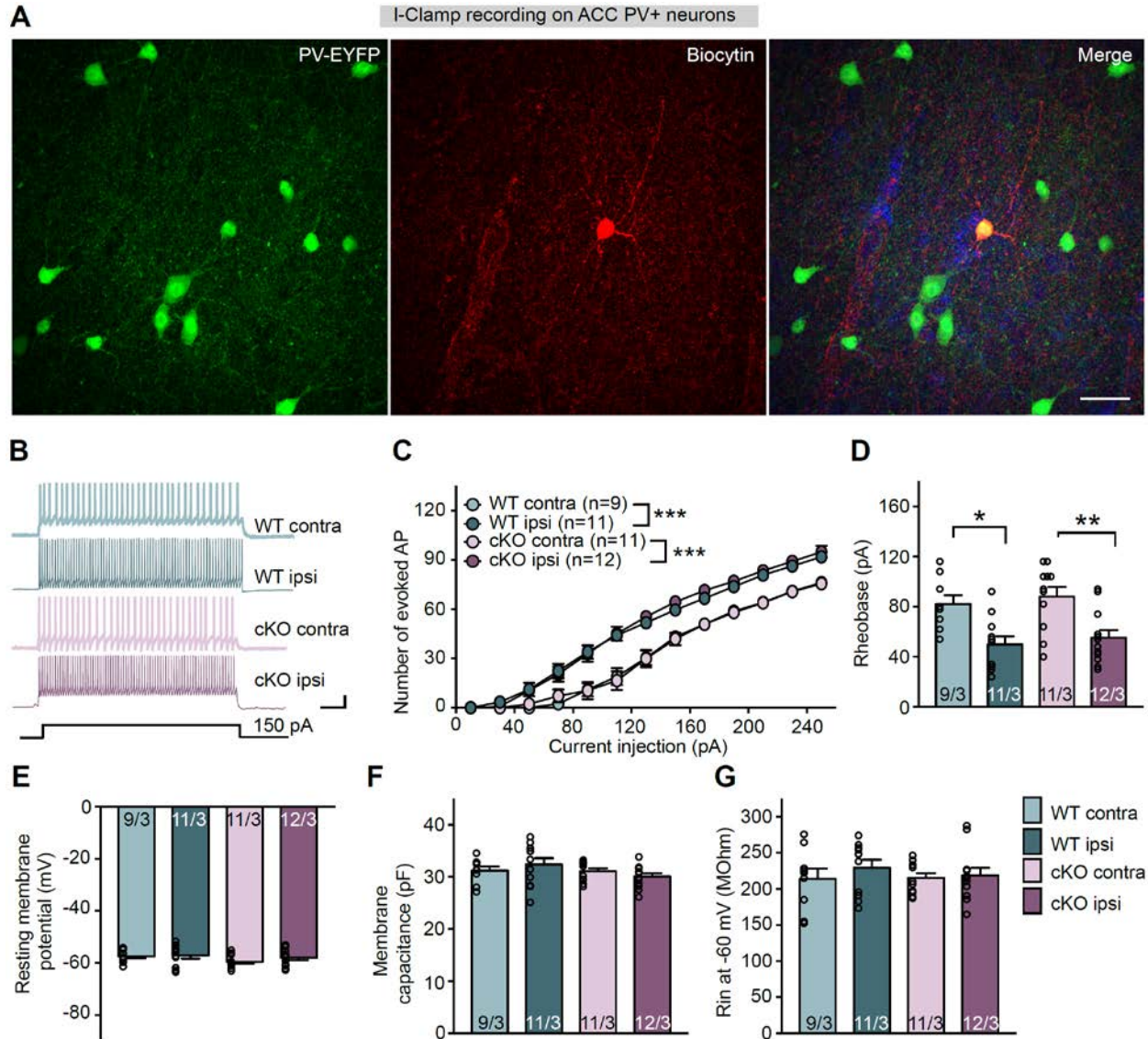
All data shown as mean ± s.e.m.

Figure S5. Spared nerve injury affects active membrane properties of PV+ cells in the ACC, related to Figures 4-6.

(A) Representative images of biocytin-labelled (red) PV+ cells, which was identified with Cre-dependent EYFP reporter expression. Scale bar: 50 μm.

(B) Sample traces of current clamp recordings from WT and RARα KO PV+ neurons ipsi- and contralateral to SNI side in response to a step current injection of 150 pA. Scale bars: 100 ms, 10 mV.

(C) Input-output relationship between the total number of APs and the step current injections. Two-way ANOVA followed by Bonferroni test, WT contra vs. ipsi: interaction (intensity × SNI) $F_{(12, 216)} = 7.10$, ***, $p < 0.001$; SNI factor, $F_{(1, 18)} = 19.15$, $p < 0.001$; cKO contra vs. ipsi: interaction, $F_{(12, 252)} = 8.90$, ***, $p < 0.001$; SNI factor, $F_{(1, 21)} = 19.79$, $p < 0.001$.

(D) Rheobase of PV+ cells at the ipsilateral and contralateral sides of WT and cKO mice. Two-way ANOVA followed by Tukey test, interaction (genotype × SNI), $F_{(1, 39)} = 0.0032$, $p = 0.98$; SNI factor, $F_{(1, 39)} = 22.23$, $p < 0.001$. Post hoc test, *, $p < 0.05$, **, $p < 0.01$.

(E-G) Quantification of passive membrane properties measured as resting membrane potentials (E), membrane capacitances (F, and input resistances (G) at -60 mV holding potential.
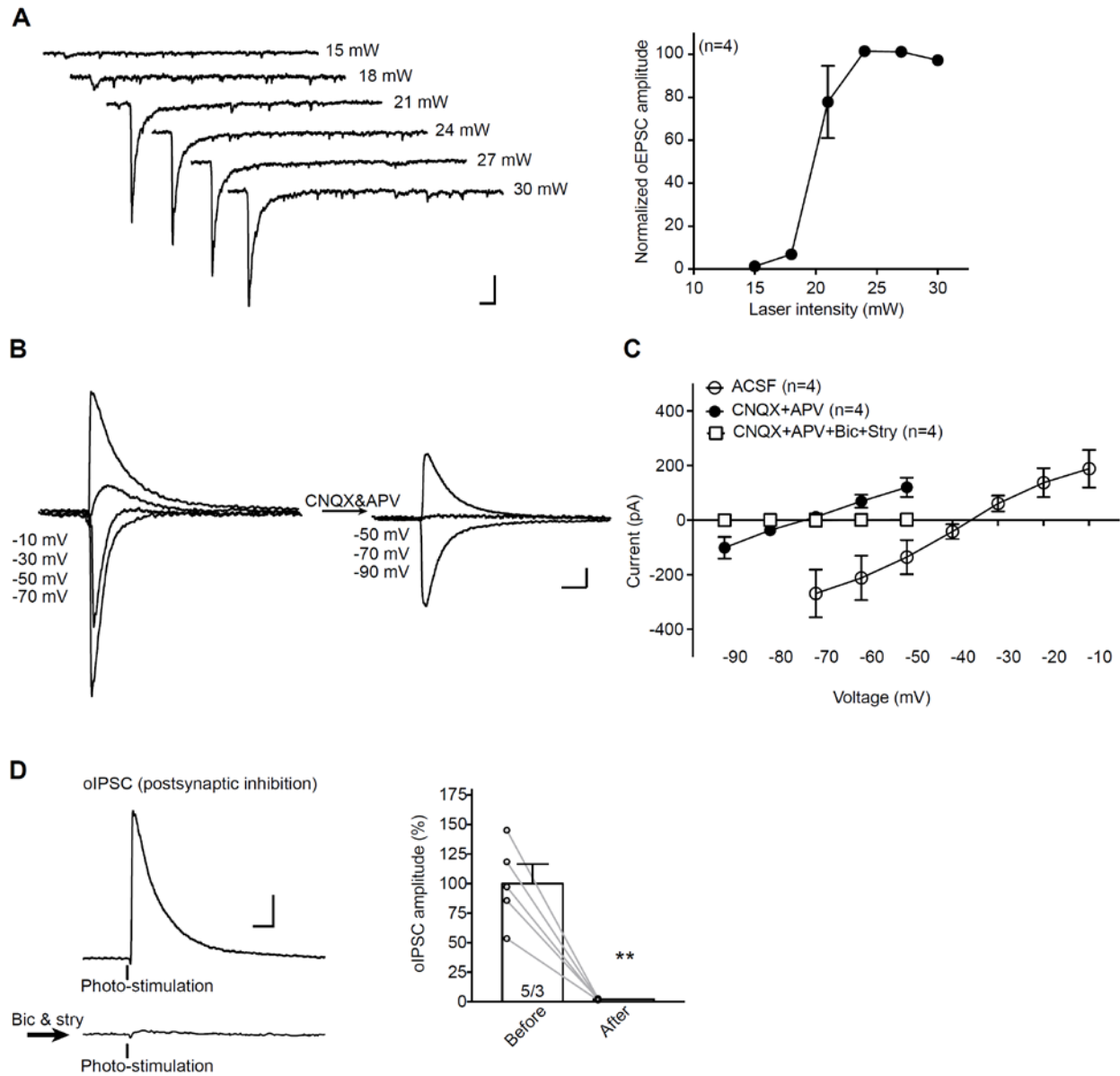
All data shown as mean ± s.e.m.

Figure S6. Pharmacological characterization of optically activated postsynaptic responses in PV+ target neurons, related to Figures 4-6.

(A) Representative traces oPSCs in response to optogenetic activation of PV+ cells at different light power (left) and input-output curves of oEPSCs from four neurons (right). Maximum responses are achieved at 25 mW and higher light power. Scale bars: 50 ms, 20 pA.

(B) Example traces of oPSCs at different membrane holding potentials in response to photo-stimulation of ChR2-expressing PV+ cells in ACSF (left) and after adding CNQX (10 µM) and APV (100 µM, right). Scale bars: 50 ms, 20 pA.

(C) I-V curve of oPSCs in ACSF, CNQX + APV and CNQX + APV + bicuculine + strychnine. In the presence of CNQX + APV, oIPSCs exhibit a reversal potential of -70 mV, and can be further blocked by bicuculine and strychnine.

(D) oIPSCs, activated by photo-stimulation of PV+ neurons, can be completely blocked by $GABA_A$ and glycine receptor antagonist bicuculline (10 µM) and strychnine (1 µM). Paired t-test, t = 6.28, **, $p < 0.01$. Scale bars: 50 ms, 20 pA.
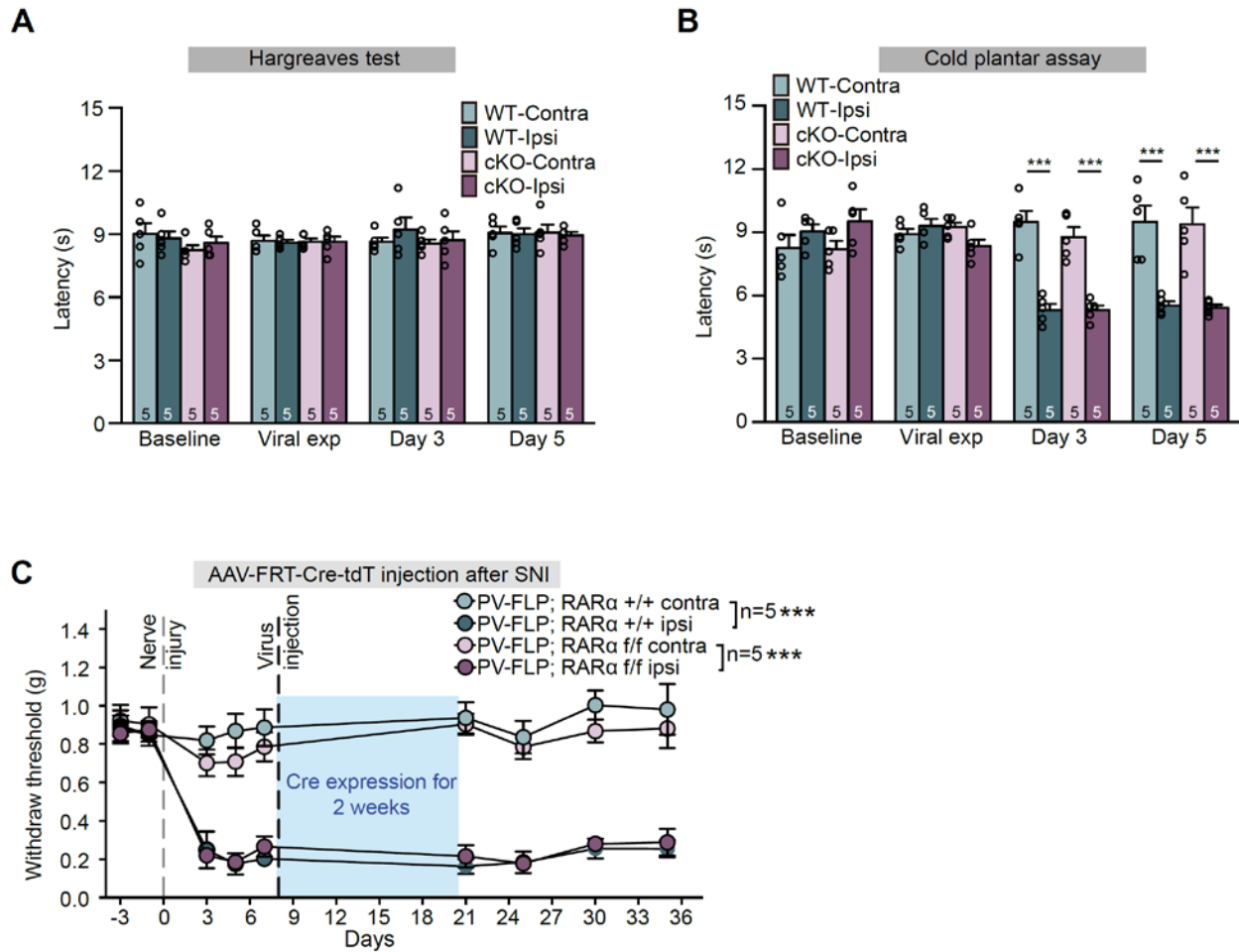
Figure S7. Region-specifically deletion of RARα in the spinal cord does not affect thermo allodynia, related to Figure 7.

(A) Heat sensitivity assessed with Hargreaves test in WT and spinal cord-specific PV-RARα deletion after SNI surgery.

(B) Cold sensitive assessed with cold plantar assay in WT and spinal cord-specific PV-RARα deletion after SNI surgery. Two-way ANOVA followed by Bonferroni test, day 3: interaction (genotype × SNI), $F(1, 16) = 0.84$, $p = 0.37$; SNI factor, $F(1, 16) = 94.11$, $p < 0.001$; Day 5: interaction, $F(1, 16) = 0.044$, $p = 0.84$; SNI factor, $F(1, 16) = 48.13$, $p < 0.001$. Post hoc test, ***, $p < 0.001$.

(C) Mechanical allodynia quantified as paw withdrawal threshold with von Frey filaments in WT and spinal-specific PV-RARα cKO mice before and after SNI. AAV-FRT-Cre-tdT was injected a week after SNI. Two-way ANOVA with Bonferroni test, WT contra vs. ipsi, interaction (days × SNI), $F(8, 64) = 10.68$, ***, $p < 0.001$; SNI factor, $F(1, 8) = 105.2$, $p < 0.001$; cKO contra vs. ipsi, interaction, $F(8, 64) = 12,13$, $p < 0.001$; SNI factor, $F(1, 8) = 57.97$, ***, $p < 0.001$. All N = # of mice. All data shown as mean ± s.e.m..

A

	Contra		Ipsi	
	Btefore	After	Before	After
WT				
cKO				

B

oEPSC amplitude (%) vs Time (Min)

WT - con
WT - ipsi
cKO-con
cKO - ipsi

Ro41-5253

C

90%-10% oEPSC decay (ms) vs Time (Min)

WT - con
WT - ipsi
cKO-con
cKO - ipsi

Ro41-5253

D

	Contra		Ipsi	
	Before	After	Before	After
WT				
cKO				

E

oIPSC amplitude (%) vs Time (Min)

WT - con
WT - ipsi
cKO-con
cKO - ipsi

Ro41-5253

F

90%-10% oIPSC decay (ms) vs Time (Min)

WT - con
WT - ipsi
cKO-con
cKO - ipsi

Ro41-5253

G

Membrane capicitance (pF)

WT-contra
WT-ipsi
cKO-contra
cKO-ipsi

8/4   8/4   8/4   8/4

Before After

H

Input resistance (MOhm)

WT-contra
WT-ipsi
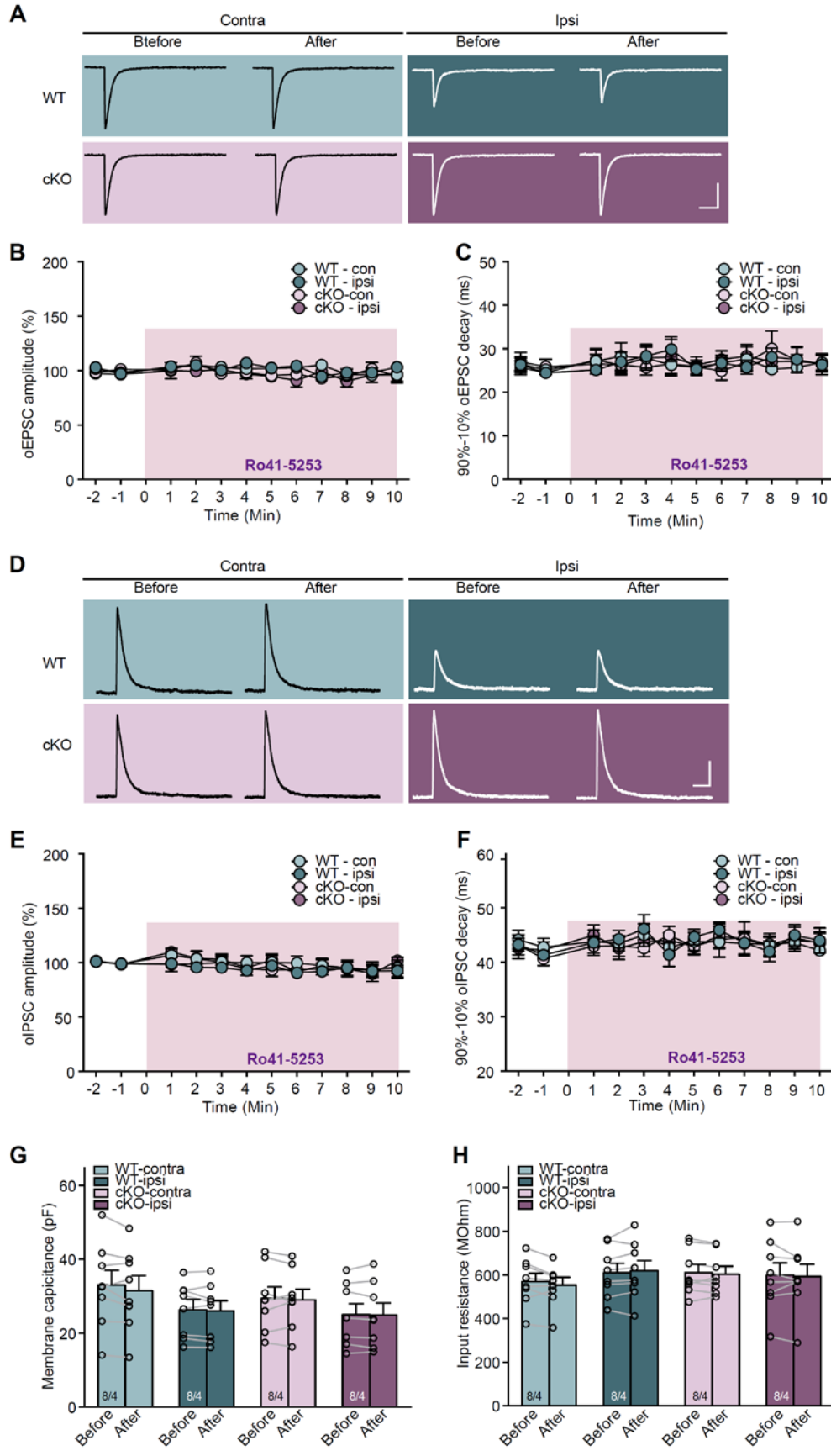cKO-contra
cKO-ipsi

8/4   8/4   8/4   8/4

Before After

Figure S8. RARα antagonist Ro41-5253 does not have acute effect on cell properties and synaptic transmission, related to Figure 8.

(A) Example traces of oEPSCs recorded from non-PV neurons in ipsilateral and contralateral sides of dorsal horn lamina IIi+III of WT and PV-RARα cKO mice with SNI before and 10 min after 0.5 mM Ro41-5253 application. Scale bars: 200 pA, 100 ms.

(B) Measurement of oEPSC amplitudes before and during Ro41-5253 application. Amplitudes are normalized to the initial (-2 min) amplitude (n = 4 cells/group).

(C) Measurement of oEPSC kinetics (90-10% decay time) before and during Ro41-5253 application (n = 4 cells/group).

(D) Example traces of oIPSCs recorded from non-PV neurons in ipsilateral and contralateral sides of dorsal horn lamina IIi+III of WT and PV-RARα cKO mice with SNI before and 10 min after 0.5 mM Ro41-5253 application. Scale bars: 100 pA, 100 ms.

(E) Measurement of oIPSC amplitudes before and during Ro41-5253 application. Amplitudes are normalized to the initial (-2 min) amplitude (n = 4 cells/group).

(F) Measurement of oIPSC kinetics (90-10% decay time) before and during Ro41-5253 application.

(G) Membrane capacitance before and 10 min after Ro41-5253 application (n = 8 cells from 4 animals per group).

(H) Input resistance before and 10 min after Ro41-5253 application (n = 8 cells from 4 animals per group).